ARTICLE IN PRESS

Estuarine, Coastal and Shelf Science xxx (xxxx) xxx

Contents lists available at ScienceDirect

Estuarine, Coastal and Shelf Science

journal homepage: http://www.elsevier.com/locate/ecss

# Beyond 2100: Elevation capital disguises salt marsh vulnerability to sea-level rise in Georgia, USA

Amy K. Langston [a,*], Clark R. Alexander [b,c], Merryl Alber [c], Matthew L. Kirwan [a]

[a] Virginia Institute of Marine Science, William & Mary, PO Box 1346, Gloucester Point, VA, 23062, USA
[b] Skidaway Institute of Oceanography, University of Georgia, Savannah, 10 Ocean Science Circle, Savannah, GA, 31411, USA
[c] Department of Marine Sciences, University of Georgia, 325 Sanford Drive, Athens, GA, 30602, USA

ARTICLE INFO

*Keywords:*
Accretion
GCE-LTER
Long-term changes
Mathematical models
Sediment sampling

ABSTRACT

Salt marshes rely on sufficient sediment inputs and room for lateral migration to maintain vertical and lateral stability under sea-level rise. As the global rate of sea-level rise accelerates, marshes unable to keep pace become vulnerable to drowning. We evaluated the long-term response of a salt marsh in Georgia, USA, to historical (1935–2018) and future projected rates of sea-level rise. We expected the marsh to be resilient because it receives high sediment inputs and has room to migrate landward. However, sediment cores show marsh accretion (1.55 mm $y^{-1}$) is lower than the historical rate of sea-level rise (3.25 mm $y^{-1}$) and that rates are independent of elevation. Results from a vertical accretion model show that while marsh area is stable through 2100 under historical and high sea-level rise scenarios, the marsh relies on elevation capital to maintain its extent under a high rate of sea-level rise. The marsh rapidly loses area beyond 2100 as it depletes its elevation reserve. By 2160, only 12% of the initial marsh area remains. Our results demonstrate that while elevation capital can extend the period of time a marsh maintains its areal extent, it does not remove the long-term threat of drowning when marsh accretion cannot keep pace with sea-level rise.

## 1. Introduction

Salt marshes provide many critical ecological functions in temperate coastal regions. They are highly productive ecosystems that protect inland regions from chronic (e.g., tidal flooding, sea-level rise) and episodic (e.g., hurricanes, storms) events by attenuating tides and storm surges (Gedan et al., 2011; Shepard et al., 2011; Leonardi et al., 2018). They are among the most important carbon sinks in the world, sequestering carbon at higher rates than any other wetland type (Zedler and Kercher, 2005; Bridgham et al., 2006; Kirwan and Mudd, 2012). Salt marshes also reduce eutrophication via nutrient cycling, reduce flooding from storm surge, support terrestrial and marine food webs, and provide nesting and refuge habitat for coastal fauna (Currin et al., 1995; Deegan and Garritt, 1997; Cloern et al., 2002; Greenberg et al., 2006; Sousa et al., 2010). Yet, marshes and their ecosystem services are threatened by sea-level rise (SLR) and other anthropogenic impacts (Kirwan and Megonigal, 2013; Crosby et al., 2016; Kirwan et al., 2016a; Schuerch et al., 2018; FitzGerald and Hughes, 2019).

Salt marshes are dynamic ecosystems that naturally adjust vertically and laterally in response to changes in sea level (Friedrichs and Perry, 2001; Morris et al., 2002; Kirwan et al., 2016b; Ganju et al., 2017). Long-term vertical marsh stability is driven by non-linear geomorphic feedbacks between sea level, sediment deposition, and organic matter accumulation that dictate rates of accretion across the marsh (Mudd et al., 2009; Kirwan and Guntenspergen, 2012; Roner et al., 2016). Accretion rates vary with elevation and distance from tidal channels across a marsh landscape. Sediment accretion is typically highest in areas that receive the most tidal inundation, namely at lower elevations and near tidal channels (Friedrichs and Perry, 2001; Temmerman et al., 2003; FitzGerald et al., 2008; Kirwan and Megonigal, 2013). Organic accretion depends on elevation and is typically highest at elevations that support maximum plant productivity (Redfield, 1972; Morris et al., 2002; Kirwan and Guntenspergen, 2012). Marshes maintain their lateral extent by migrating landward as flooding frequency increases (Langston et al., 2017; Schieder et al., 2018; Kirwan and Gedan, 2019). To be resilient to SLR, a salt marsh must receive sufficient sediment inputs to maintain elevations within ranges that support marsh vegetation, and migrate landward at a rate that offsets edge erosion (Cadol et al., 2014;

* Corresponding author.
*E-mail addresses:* aklangston@vims.edu (A.K. Langston), clark.alexander@skio.uga.edu (C.R. Alexander), malber@uga.edu (M. Alber), kirwan@vims.edu (M.L. Kirwan).

https://doi.org/10.1016/j.ecss.2020.107093
Received 3 April 2020; Received in revised form 3 November 2020; Accepted 9 November 2020
Available online 17 November 2020

Kirwan et al., 2016b; Alexander et al., 2017; Schuerch et al., 2018).

Human-induced and natural disturbances can disrupt the geomorphic processes by which salt marshes maintain stability under a rising sea level. Dams upstream of estuaries reduce downstream sediment inputs, potentially limiting rates of mineral accretion (Syvitski et al., 2005; Kirwan et al., 2010; Weston, 2014). Grazing by marsh invertebrates, wrack accumulation, and other disturbances reduce plant productivity and organic accretion (Alber et al., 2008; Deegan et al., 2012; Crotty et al., 2017; Angelini et al., 2018). Additionally, barriers such as infrastructure, shoreline protection, and steep slopes limit marsh migration into adjacent uplands (Enwright et al., 2016; Kirwan et al., 2016b; Dugan et al., 2018; Gehman et al., 2018; Schuerch et al., 2018; Thorne et al., 2018).

Due to their biophysical characteristics, marshes are considered most resilient to SLR under conditions of high sediment supply, tidal range, and availability of land for marsh migration (Kirwan et al., 2010, 2016b; Kearney and Turner, 2015). When those conditions do not allow for marsh sustainability, marshes must instead rely on "elevation capital" to prolong their survival. Coined by Reed (2002), the term "elevation capital" describes the elevation of the marsh above that which is required for vegetation growth. Sediment and organic material accumulated during marsh formation and other periods of soil growth form a reserve that is then depleted when vertical accretion is outpaced by SLR (Reed, 2002; Cahoon and Guntenspergen, 2010; Cahoon et al., 2019; Langston et al., 2020). Marshes with high elevation capital may survive for decades to centuries, even when sediment balances are negative (i.e. sedimentation fails to keep pace with SLR and erosion), and the marsh becomes closer to submergence (Ganju et al., 2017; Langston et al., 2020). Marshes that rely on elevation capital may appear stable under accelerated rates of SLR for decades or more, but on longer timelines are

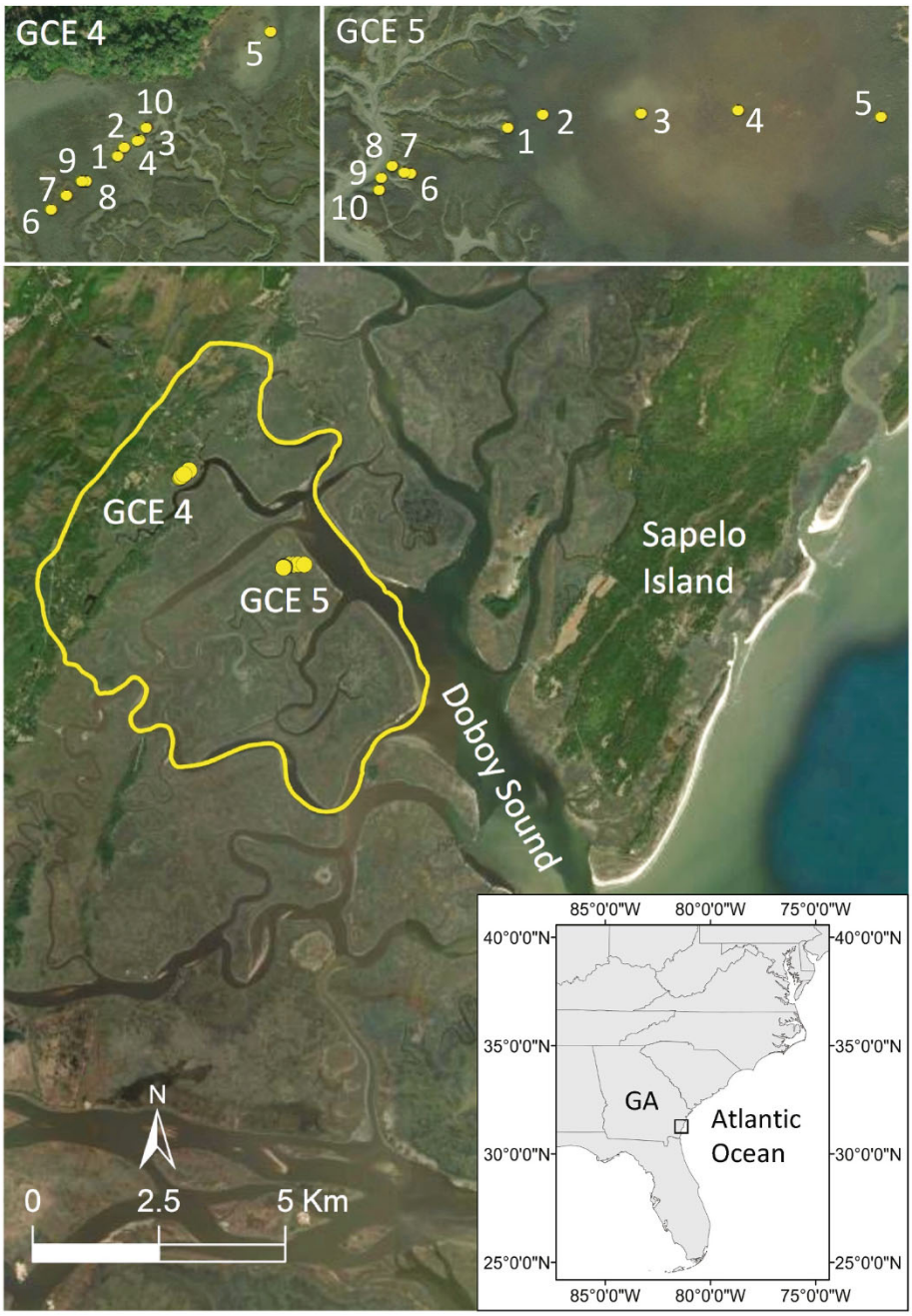


**Fig. 1.** Location map of salt marsh study area within the GCE LTER, Georgia, USA. Insets show the sediment cores (labeled 1–10) along elevation transects in GCE 4 and GCE 5.

susceptible to rapidly drowning when their elevation capital is depleted. Therefore, recognizing the contribution of elevation capital is especially valuable when predicting long-term marsh survival under different projections of SLR.

Although many landscape-scale numerical models explore how ecogeomorphic feedbacks influence the stability of intertidal marshes over the current century (e.g., Schile et al., 2014; Swanson et al., 2014; Alizad et al., 2016; Cadol et al., 2016; Wu et al., 2017; Langston et al., 2020), the fate of marshes after 2100 remains largely unexplored. Here, we evaluate the response of a salt marsh in the Georgia Coastal Ecosystems (GCE) Long-term Ecological Research Site (LTER; USA) to SLR by measuring historical sediment accumulation rates and applying a numerical model of marsh accretion. Although we anticipated marsh stability in this sediment rich, gently sloping system, we found instead that the marsh relied on elevation capital to survive SLR through 2100, but was vulnerable to drowning beyond 2100.

## 2. Methods

### 2.1. Study site

Our study marsh is located on Doboy Sound southwest of Sapelo Island, GA, USA, and is within the domain of the GCE LTER, which has a series of salt marsh monitoring sites that are representative of South Atlantic tidal wetlands (Pennings et al., 2012). The study took place in a 40 $km^2$ area ('GCE marsh') that encompasses two of these long-term sites (GCE 4 and 5), which have been sampled since 2000 (Wieski and Pennings, 2014). It includes 24 $km^2$ of vegetated marsh dominated entirely by *Spartina alterniflora* (smooth cordgrass; Fig. 1). Tributaries of Doboy Sound create dense networks of channels within the study area; tidal flats are common near tributaries at low elevation and at the marsh-upland boundary (Burns et al., 2020). Uplands adjacent to the marsh have shallow slopes (average 2.24 ± 2.2° over 50 m; Burns et al., 2020) and support coniferous forest, forested wetlands, and low intensity urban land use. Mean elevation of the marsh is approximately 0.77 m relative to mean sea level (MSL; Burns et al., 2020). The GCE receives high sediment inputs from the Altamaha River; mean suspended sediment concentration is approximately 40 mg $L^{-1}$. The region is mesotidal (mean tidal range ~2 m) and the long-term historical rate of SLR is 3.25 mm $y^{-1}$ (1935–2018; Fort Pulaski #8670870).

### 2.2. Sediment cores

Sediment cores were collected at GCE LTER sampling sites, GCE 4 and GCE 5, to characterize long-term sediment accumulation with respect to marsh elevation (Fig. 1). Ten cores were collected along an elevation transect at each site, for a total of 20 cores. Coring site elevations ranged from about MSL to 1 m above MSL. Cores 30–50 cm long were collected in 15-cm diameter PVC barrels, returned to the lab, and extruded at 1-cm intervals for $^{210}$Pb geochronology. Long-term (100-y timescale) sediment accumulation rates were determined using $^{210}$Pb, a naturally occurring radionuclide. Samples were dried, ground, sealed in Nalgene jars, equilibrated for a month, and counted for 24 h on a planar germanium detector to develop profiles of the activities (dpm $g^{-1}$) of total $^{210}$Pb and supported $^{210}$Pb (from $^{226}$Ra through its daughter products $^{214}$Pb and $^{214}$Bi) (Alexander and Venherm, 2003). Subtracting supported $^{210}$Pb from total $^{210}$Pb yields excess $^{210}$Pb, the decay of which is mathematically related to the sediment accumulation rate. Sediment accumulation rates were determined from the slope of the regression line through the excess $^{210}$Pb data points created by decay of excess $^{210}$Pb in the seabed. Steep slopes indicated rapid accumulation and shallow slopes indicated slow accumulation rates. In many cases biological and/or physical processes rapidly mix the uppermost seabed; hence, the accumulation rate was determined using the decay profile of excess $^{210}$Pb below this mixed surface layer (DeMaster et al., 1985). $^{210}$Pb rates were verified by identification of the 1963 maximum input peak of $^{137}$Cs, a bomb-produced tracer associated with atmospheric weapons testing. See Alexander and Venherm (2003) for further details of radiochemical techniques.

### 2.3. Model description

We applied a spatially-explicit vertical accretion model (Duran Vinent et al., 2019; Langston et al., 2020) to predict responses of the GCE marsh to scenarios of SLR. Following Langston et al. (2020), the model considers the evolution of marsh vegetation and elevation relative to SLR through time. In the model, marsh vegetation occupies a site-specific range of elevations suitable for vegetation growth (see Section 2.3.3 on model parameterization), and changes in vegetation coverage (i.e., conversion of high to low marsh, marsh to open water, migration into uplands) are calculated with a decadal timestep. For marshes supporting multiple vegetation types, the model can account for the contributions of organic material from each dominant plant species across elevation zones as well as changes in species composition that accompany changes in elevation, as demonstrated in Langston et al. (2020). Changes in salt marsh elevations are calculated on an annual timestep according to the mass balance between rates of mineral accretion and organic accretion:

$$\frac{\partial Z}{\partial t} = A_m(x,y,Z) + A_o(x,y,Z) - R \tag{1}$$

where mineral accretion, $A_m$, is a function of elevation and distance from the nearest channel at location (x,y), organic accretion, $A_o$, is a function of elevation only, and $R$ is the rate of relative SLR. Following Langston et al. (2020), we do not consider the lateral erosion of marsh edges, the evolution of unvegetated portions of the landscape, such as tidal channels, ponds, and mudflats, nor the effects of storms or other stochastic events. Though beyond the scope of this model, these processes are important in marsh development and stability, and have been addressed in other models (e.g.,(Kirwan et al., 2016b; Ganju et al., 2017; Van der Wegen et al., 2019; Mariotti, 2020).

#### 2.3.1. Mineral accretion

Mineral accretion is calculated using a simplified 1D transport model (Duran Vinent et al., 2019) in which rates of $A_m$ decrease with distance, $l$, from the nearest channel:

$$A_m(x,y,Z) = A_m^{max}(Z)e^{\frac{l(x,y)}{L_c}} \tag{2}$$

where $A_m^{max}$ is a reference accretion rate, and length, $L_c$, describes the spatial decay of $A_m$. Based on mass conservation, $A_m^{max}$ is proportional to the suspended sediment concentration at the marsh edge ($C_0$), an effective falling velocity, $w_f$, and the rescaled local inundation time, $\tau(Z)$:

$$A_m^{max}(Z) = \frac{C_0 w_f}{\rho_m}\tau(Z)\, r\left(\frac{w_f T}{\delta z}\right) \tag{3}$$

where $\rho_m$ is the density of mineral sediments deposited on the marsh, $\tau(Z) = \pi^{-1}\cos^{-1}(2Z/\delta z)$, and $r$ is a fitting function with values between 0.5 and 1 that represents the effect of sediment inertia on the temporal decrease of suspended sediments during ebb flows. The decay length, $L_c$, scales with the ratio of tidal water discharge per unit width and $w_f$:

$$L_c = \beta\left(\frac{L\delta z}{T w_s}\right) \tag{4}$$

where $L(x, y)$ is the length of the local drainage basin, $T$ is the tidal period, $w_s$ is the settling velocity, and $\beta$ is a fitting parameter (1.5).

#### 2.3.2. Organic accretion

Organic accretion ($A_o$) is a function of above- and belowground biomass of the dominant plant species, *S. alterniflora*:

$$A_o(x, y, Z) = \frac{kBP}{\rho_o} \quad (5)$$

where $k$ is the recalcitrant fraction of belowground biomass, $B$ is the ratio of below- to aboveground biomass of *S. alterniflora*, $P$ is the aboveground biomass of *S. alterniflora*, and $\rho_o$ is the density of pure organic sediments. Aboveground biomass depends on elevation, as defined by a parabolic function (Morris et al., 2002):

$$P(x, y, Z) = aZ + bZ^2 + c \quad (6)$$

where $a$, $b$, and $c$ are locally derived coefficients that determine upper and lower elevation limits of biomass for *S. alterniflora*.

### 2.3.3. Model parameterization

We parameterized the model using spatial data, sediment core data, and the literature (Table 1). We used a vegetation-corrected digital elevation model (DEM) developed from 2009 LiDAR and referenced to NAVD88 (Hladik and Alber, 2012) and a 2013 habitat raster to define initial elevations and habitat distributions in the model domain. Before running the model, we converted the spatial resolution of the DEM from 4.6 $m^2$ to 10 $m^2$, consistent with the resolution of the habitat raster, and converted the vertical datum to MSL. All reported elevations are relative to MSL. The model includes all three habitat types present in the study site: vegetated marsh dominated by *S. alterniflora*, water, and upland. We created a probability distribution of *S. alterniflora* using the DEM and habitat raster to identify minimum and maximum elevation limits of the marsh. Elevation limits were defined as the elevations where the probability of *S. alterniflora* occurrence was ~50%. The elevation for peak aboveground biomass (0.45 m) was the midpoint of the marsh elevation range (−0.51-1.39 m). We used a below- to aboveground ratio of 0.4, consistent with the median value of root:shoot field measurements collected in the GCE LTER (J. O'Connell; personal communication).

### 2.3.4. Model sensitivity and uncertainty

In a previous study, we found that this model was most sensitive to suspended sediment concentration, maximum aboveground biomass, and DEM elevation error (Langston et al., 2020). To account for uncertainty and natural variation in mineral and organic accretion parameters, we used a range of values for suspended sediment concentration and maximum aboveground biomass. Suspended sediment concentration values ranged from 26 to 62 mg $L^{-1}$, spanning median spring and fall suspended sediment concentrations measured in marsh and levees within the study area, and include suspended sediment concentration from Hurricane Irma in 2017 (Wiberg et al., 2018). Maximum aboveground biomass values ranged from 500 to 2500 g $m^{-2}$, informed by minimum and maximum end-of-year biomass measured in the creekbank zone at GCE 4 and GCE 5 from 2000 to 2011 (Wieski and Pennings, 2014). We also applied a DEM error term ($E_{DEM}$) to account for potential discrepancies within ±0.2 m between the DEM and ground elevations (Bater and Coops, 2009; Hladik and Alber, 2012).

### 2.3.5. Model experiments

We predicted the response of the GCE marsh to two scenarios of SLR: historical (3.25 mm $y^{-1}$) and high (18.9 mm $y^{-1}$ in 2100). The historical SLR scenario represented a low SLR scenario in which the current rate of SLR was maintained over time. Under the high SLR scenario, the rate of SLR accelerated over time, following IPCC RCP scenario 8.5 (IPCC, 2013), and was adjusted for local subsidence inferred from the Fort Pulaski, GA tide station (1935–2018). This scenario represented likely future conditions based on current greenhouse gas emissions. For each scenario of SLR, we tested marsh response under two accretion scenarios: spatially-variable accretion dependent on elevation, and a constant accretion rate, regardless of elevation. The former accretion scenario reflected typical non-linear dynamics between sediment deposition, primary productivity, and inundation (Morris et al., 2002; Kirwan and Megonigal, 2013). The constant accretion rate was equivalent to the mean accretion rate calculated from core measurements (1.55 mm $y^{-1}$) from GCE 4 and GCE 5, which showed no relationship between sediment accumulation and elevation (Fig. 2). We evaluated marsh response under all four scenarios on an annual time step (t = 88) for 2013–2100, and on an extended timeline spanning 2013–2400. The projection for the high SLR scenario was extended to 2400 using a polynomial equation derived from 2013 to 2100 MSL data, and represents a scenario in which MSL continues along the same trajectory from 2013 to 2400. Uncertainty was incorporated into the model by including a range of input values for $C_0$, $P_{max}$, and $E_{DEM}$ (Table 1); values for each model run were randomly generated from uniform distributions bounded by range limits described above in Section 2.3.4. Unless otherwise stated, results are presented as mean values based on 50 model runs ±1 standard deviation.

**Table 1**
Model parameters.

| Parameter | Value | References |
|---|---|---|
| *Mineral Accretion ($A_m$)* | | |
| $C_0$ | 26–62 mg $L^{-1}$ | Wiberg et al. (2018) |
| $w_s$ | $2.7 \times 10^{-6}$ m $s^{-1}$ | |
| $\rho_m$ | $1.99 \times 10^6$ g $m^{-3}$ | Morris et al. (2016) |
| *Organic Accretion ($A_o$)* | | |
| $P_{max}$ | 500–2500 g $m^{-2}$ | Wieski and Pennings (2014) |
| B | 0.4 | Pers. Comm. (J. O'Connell) |
| K | 0.1 | Benner et al. (1984) |
| $\rho_o$ | 8.5 × 104 g $m^{-3}$ | Morris et al. (2016) |

## 3. Results

### 3.1. Sediment cores

In general, well-behaved excess $^{210}$Pb decay profiles in the marsh cores suggest that they preserve an undisturbed record of sediment accumulation (Fig. 3). Sediment accumulation rates within the GCE study site ranged from 0.3 to 4.1 mm $y^{-1}$ (0.01–0.17 g $cm^{-2}$ $y^{-1}$) and averaged 1.55 mm $y^{-1}$ (0.07 g $cm^{-2}$ $y^{-1}$), indicating that these marshes did not keep up with the local historical rate of SLR. Although most rates were below 2 mm $y^{-1}$, the highest rate of accumulation (4.1 mm $y^{-1}$)

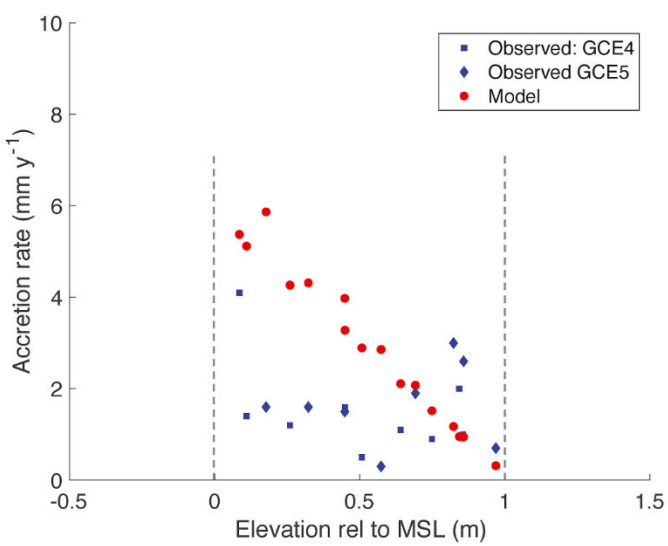


**Fig. 2.** Comparison of sediment accumulation rates from $^{210}$Pb sediment cores (blue squares and diamonds) and modeled accretion rates (red circles) across elevation relative to MSL. Core samples were collected from GCE 4 and GCE 5 LTER sampling sites (n = 20). Dashed lines mark MSL (0 m) and MHW (1.01 m). (For interpretation of the references to colour in this figure legend, the reader is referred to the Web version of this article.)

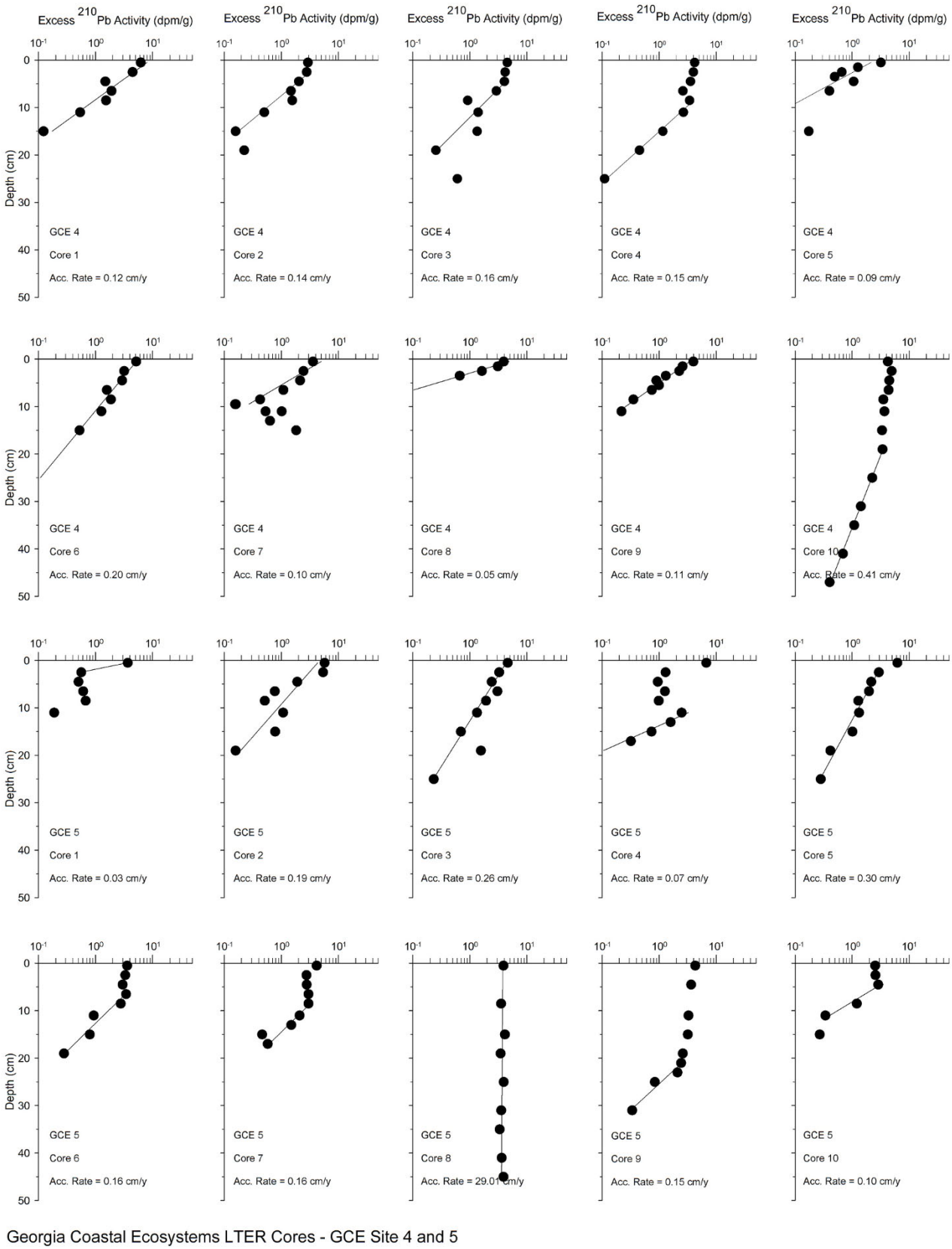


**Fig. 3.** $^{210}$Pb profiles of sediment cores in GCE 4 and GCE 5. Accumulation rate is determined by the slope of the line through the excess $^{210}$Pb data points below the mixed surface layer. Steep slopes denote rapid accumulation (e.g., GCE 4, core 10; GCE 5, core 8) whereas gentle slopes denote slow rates (e.g., GCE 4, core 9; GCE 5, core 4). The uppermost seabed is often rapidly mixed by biological and/or physical processes, and only the decay profile of excess $^{210}$Pb below this mixed layer is considered in determining accumulation rates (e.g., GCE 4, core 4; GCE 5, core 6).

was observed in the core from the lowest elevation. Nevertheless, there was no clear trend in accretion rates with elevation, as a peak was also observed in cores from approximately 0.8 m above MSL, which is slightly lower than the location of mean high water (MHW) in this area (1.01 m).

### 3.2. Model

Accretion rates in the GCE study site did not keep pace with historical or high rates of SLR, regardless of the relationship between accretion and elevation (Fig. 4a). When accretion depended on elevation, total accretion (mineral and organic) increased to 2.56 ± 0.49 mm $y^{-1}$ by 2100 under the historical SLR scenario, compared to 2.01 ± 0.82 mm $y^{-1}$ in 2013. Under the high SLR scenario (18.9 mm $y^{-1}$ in 2100), accretion increased to 6.27 ± 1.1 mm $y^{-1}$. Accretion rates under both historical and high SLR scenarios were highest near interior channels (Fig. 5a). As rates of SLR outpaced accretion rates, marsh elevation relative to sea level decreased over time (Fig. 4b). Under the historical SLR scenario, elevation decreased from 0.77 ± 0.1 m to 0.69 ± 0.07 m by 2100 when accretion depended on elevation, and to 0.64 ± 0.11 m when accretion across the marsh was fixed at 1.55 mm $y^{-1}$. Under the high SLR scenario, elevation decreased to 0.11 ± 0.08 m when accretion depended on elevation and to −0.01 ± 0.1 m when accretion was constant.

Despite decreases in elevations over time (Fig. 4b), the GCE marsh maintained its areal extent under all SLR scenarios through 2100 (Fig. 5b). Under the historical SLR scenario, the area of vegetated marsh remained the same (23.5 ± 0.39 $km^2$) in 2013 and 2100 when accretion depended on elevation, and decreased slightly to 23.2 ± 0.39 $km^2$ when accretion was constant (Fig. 6). Marsh extent increased to 24.1 ± 0.44 $km^2$ under a high rate of SLR when accretion depended on elevation, and decreased to 22.1 ± 0.59 $km^2$ when accretion was constant. Over longer simulations (2013–2400), the model showed that marsh area remained stable under the historical rate of SLR, regardless of accretion scenario (Fig. 6). However, under the high SLR scenario, marsh area declined rapidly after 2130. Marsh loss occurred at similar rates with and without elevation-dependent accretion. Model results for elevation-dependent accretion showed marsh area decreased 50% by 2142 (Fig. 7). Marsh area decreased 75% by 2148 and 88% by 2157, before stabilizing at 2.5–3.6 $km^2$ for nearly 100 years (Fig. 6). The marsh decreased to 10% of its 2013 extent in 2253 (Fig. 7). Less than 1 $km^2$ of marsh remained in 2277, and by 2343, 100% of the marsh drowned.

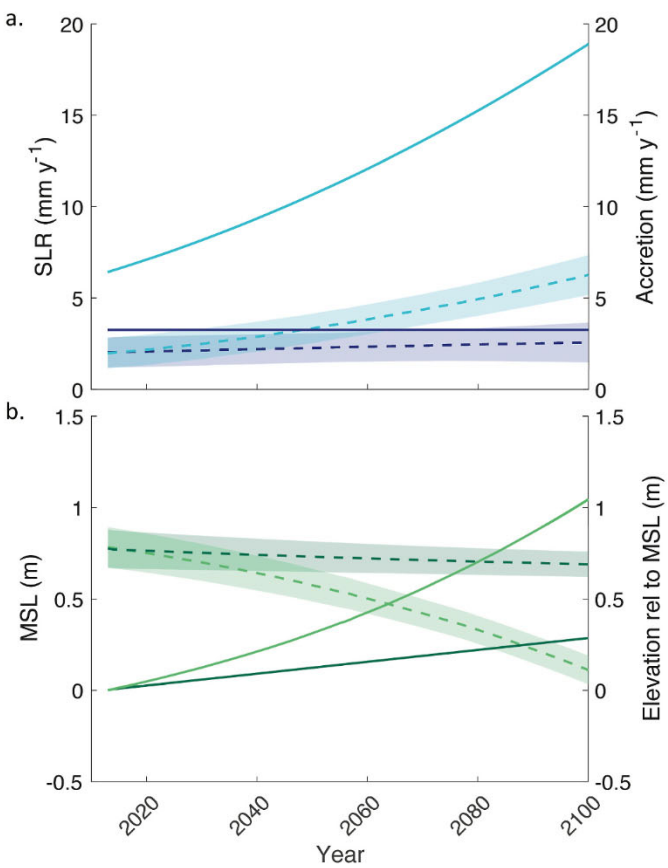


**Fig. 4.** Modeled a) accretion rate (dashed dark blue) over time under the historical rate of SLR (solid dark blue), and accretion rate (dashed light blue) over time under the high rate of SLR (solid light blue); b) elevation (dashed dark green) and MSL (solid dark green) over time under the historical rate of SLR, and elevation (dashed light green) and MSL (solid light green) over time under the high rate of SLR. Accretion rates and elevations are based on scenarios with dynamic accretion rates and presented as mean values ± 1 SD from n = 50 model runs. (For interpretation of the references to colour in this figure legend, the reader is referred to the Web version of this article.)

## 4. Discussion

The GCE marsh is a relatively undisturbed system that receives high sediment inputs from the Altamaha River (Trimble, 1974, 2008; Meade, 1982; Dame et al., 2000; Weston, 2014). As such, we expected mineral accretion to drive vertical accretion and to be sufficiently high for accretion rates to equilibrate with rates of SLR. However, sediment core data indicate that current rates of marsh accretion are generally < 2 mm $y^{-1}$ (Fig. 3), lagging behind the historical rate of SLR by more than 1 mm $y^{-1}$. Reported long-term accretion in the same region of the GCE LTER shows similarly low rates (Craft, 2007; Crotty et al., 2020). Core data also revealed that vertical accretion was not a simple function of elevation, with peaks near both the minimum and maximum range of marsh elevation (Fig. 3). Relatively high accretion rates in marshes near MHW is consistent with previous work on the Georgia coast (Alexander et al., 2017). Marsh accretion rates elsewhere typically increase with flooding duration (i.e., increase with decreasing elevation; Friedrichs and Perry, 2001; Kirwan and Megonigal, 2013) which is a fundamental premise of most salt marsh evolution models (e.g., Fagherazzi et al., 2012). It is unclear why vertical accretion is not correlated with elevation in the GCE marsh; insight into this dynamic warrants further investigation.

Low rates of vertical accretion despite high sediment availability suggests a limited portion of available sediment is deposited on the GCE marsh, and/or that other processes are interfering with lateral sediment transport across the marsh. For example, marshes exposed to waves have maximum accretion rates at slightly higher elevations (Duvall et al., 2019), and sediment accretion in the interior of marshes can become decoupled from conditions near the marsh edge (Coleman et al., 2020). Although soils in the GCE are dominated by mineral sediment (typically > 90% by mass), declines in plant biomass at the GCE may also be affecting measured accretion rates. Reductions in aboveground biomass have been observed in marshes at the GCE LTER in association with extended periods of drought and exacerbated by grazing invertebrates (Alber et al., 2008; O'Donnell and Schalles, 2016; Angelini et al., 2018). Reduced aboveground biomass not only limits rates of organic accretion, but also indirectly limits rates of sediment accretion by minimizing the facilitating role marsh vegetation plays in slowing velocities of tidal water and trapping sediments (Nyman et al., 2006; D'Alpaos et al., 2007; Li and Yang, 2009; Coleman and Kirwan, 2019). Decreased biomass may also contribute to the weak relationship between accretion and elevation; die-back events from droughts and grazing likely disrupt simple relationships between plant productivity and elevation (Morris et al., 2002).

Regardless of the relationship between accretion and elevation, our modeling offers several important insights. First, the GCE marsh was able to survive accelerated rates of SLR through 2100 because it sits fairly high in the tidal range and therefore has sufficient elevation

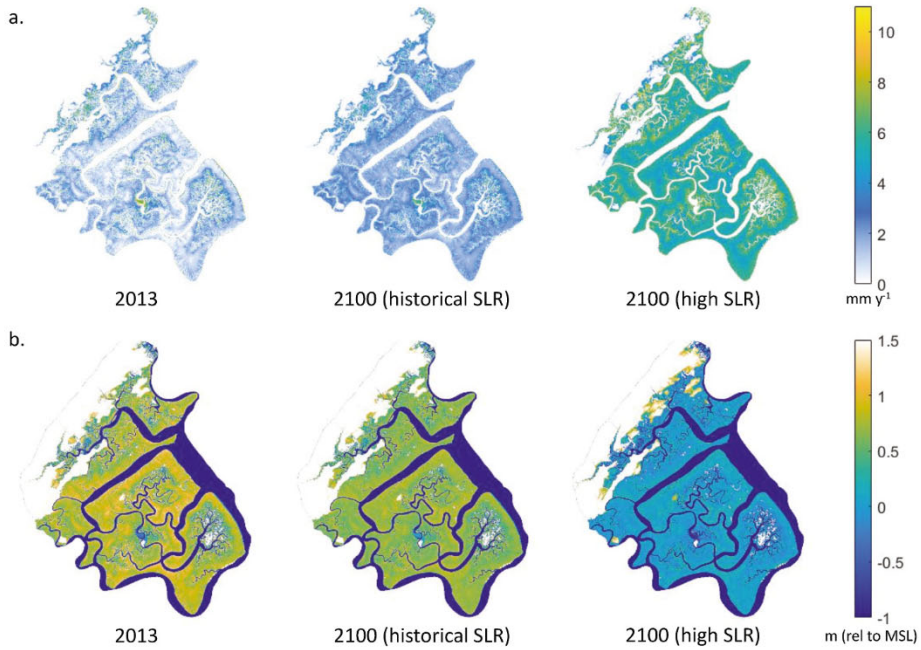


**Fig. 5.** Spatial distributions of a) accretion rates and b) elevation across the GCE marsh in 2013 (t = 0) and in 2100 under historical and high SLR scenarios.

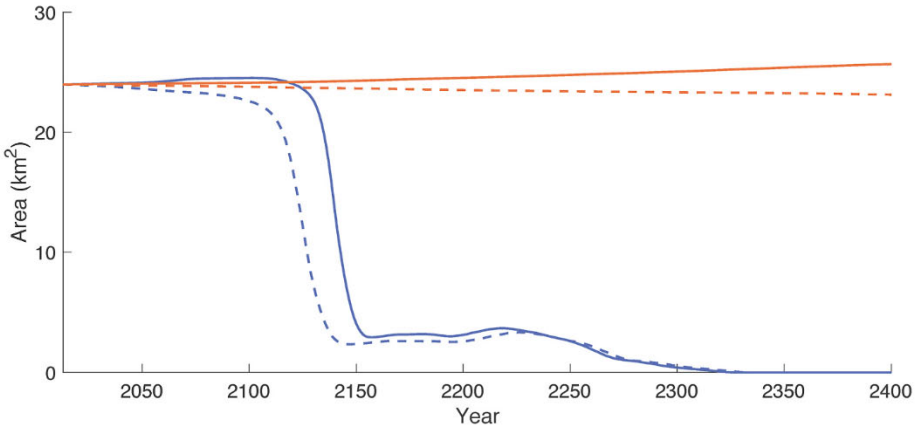


**Fig. 6.** Modeled salt marsh extent under historical (orange) and high SLR (blue) scenarios through 2400. The solid lines denote model results with dynamic marsh accretion, whereas the dashed lines denote model results with a fixed accretion rate. (For interpretation of the references to colour in this figure legend, the reader is referred to the Web version of this article.)

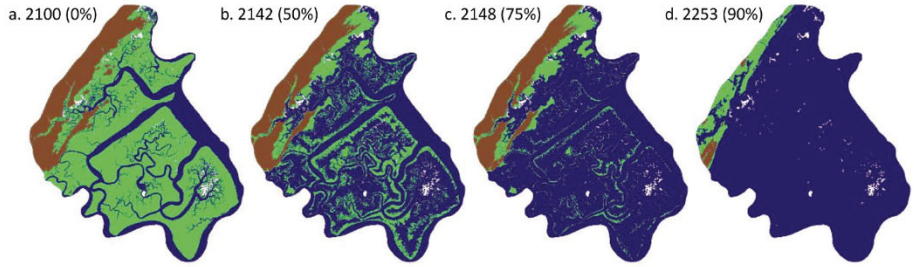


**Fig. 7.** Pattern of marsh drowning under the high SLR scenario and elevation-dependent accretion as marsh loss increases from 0 to 90% between 2100 and 2253 (marsh = green, water = blue, upland = brown, unvegetated mudflats excluded from model = white). (For interpretation of the references to colour in this figure legend, the reader is referred to the Web version of this article.)

capital to withstand accelerated inundation (Figs. 4 and 5). This behavior is consistent with historical photograph analysis at the site showing little change in marsh area through time (Burns et al., 2020). Elevation capital provides a reserve of elevation that allows the GCE marsh to maintain its extent and survive increased flooding despite low accretion rates relative to the rate of SLR (Crotty et al., 2020). The

importance of elevation capital has previously been shown in marshes in the Northeastern United States. Elevation capital sustained survival of marshes in Jamaica Bay, NY, and Narragansett Bay, RI, while lower elevation marshes in the same regions deteriorated (Watson et al., 2017; Cahoon et al., 2019). Elevation capital even prolongs the survival of marshes considered the most vulnerable to drowning, such as those in the Plum Island Estuary, MA, where sediment inputs and room for landward migration are limited (Langston et al., 2020).

Critically, our model predictions illustrate that elevation capital does not remove the threat of marsh drowning. If accretion rates cannot keep pace with the rate of SLR, even marshes at higher elevations become vulnerable to drowning when their elevation capital is depleted (Reed, 1995; Kirwan et al., 2010; Day et al., 2011). The GCE marsh is predicted to lose 86–99% of its elevation capital by 2100 under a high rate of SLR (Fig. 4b). Generally, decreases in elevation lead to faster accretion rates as more frequent tidal flooding increases sediment deposition (Kirwan and Megonigal, 2013; Kirwan et al., 2016a). However, predicted increases in accretion accompanying declines in elevation in the GCE marsh would be insufficient to stabilize marsh elevation relative to MSL (Fig. 4). The consequences of elevation loss in the GCE marsh are not apparent by 2100 because the areal extent of the marsh remains the same as in 2013. Loss of elevation capital in many marsh systems is accompanied by changes in vegetation type, i.e., conversion from high marsh dominated by *S. patens* to low marsh dominated by *S. alterniflora* (Warren and Niering, 1993; Donnelly and Bertness, 2001; Watson et al., 2016; Langston et al., 2020). In contrast, the GCE marsh is dominated by a low marsh species, *S. alterniflora*, so changes in vegetation type will not accompany the depletion of elevation capital and warn of impending marsh loss. However, once elevation capital is depleted, marsh drowning would occur quickly; 88% of the GCE marsh is expected to drown within 60 years beyond 2100 (Figs. 6 and 7).

Our observations of substantial marsh drowning beyond 2100 illustrate that elevation capital delays, but does not prevent, marsh submergence. We recognize that increased uncertainty accompanies projections that extend far into the future, and that implementing adaptative management actions for time scales spanning generations is challenging. Nevertheless, our findings demonstrate that looking beyond 2100 offers critical insight into marsh survival not apparent on shorter timelines. Although 2100 is the standard endpoint for evaluating long-term effects of SLR on salt marshes, we recommend future modeling efforts examine marsh responses on longer timelines to gain a more complete understanding of marsh survival and vulnerability.

## CRediT authorship contribution statement

**Amy K. Langston:** Methodology, Validation, Formal analysis, Investigation, Data curation, Writing - original draft, Visualization. **Clark R. Alexander:** Methodology, Formal analysis, Investigation, Resources, Data curation, Writing - review & editing, Funding acquisition. **Merryl Alber:** Resources, Writing - review & editing, Funding acquisition. **Matthew L. Kirwan:** Conceptualization, Methodology, Resources, Writing - review & editing, Supervision, Funding acquisition.

## Declaration of competing interest

The authors declare that they have no known competing financial interests or personal relationships that could have appeared to influence the work reported in this paper.

## Acknowledgments

We thank Christine Hladik for the corrected DEM, Christine Burns for the habitat base map, Pat Wiberg for providing suspended sediment concentration data, and Jessica O'Connell for providing root:shoot biomass data. We thank Orencio Durán Vinent and Ellen Herbert for their contributions in developing the model used in this study. This work was supported by NSF Coastal SEES (#1426981), NSF LTER (OCE-1832178, DEB-1832221), NSF GLD (#1529245), and NSF CAREER (#1654374). This is Contribution No. 3968 of the Virginia Institute of Marine Science, William & Mary.

## References

Alber, M., Swenson, E.M., Adamowicz, S.C., Mendelssohn, I.A., 2008. Salt marsh dieback: an overview of recent events in the US. Estuar. Coast Shelf Sci. 80, 1–11. https://doi.org/10.1016/j.ecss.2008.08.009.

Alexander, C.R., Hodgson, J.Y.S., Brandes, J.A., 2017. Sedimentary processes and products in a mesotidal salt marsh environment: insights from Groves Creek, Georgia. Geo Mar. Lett. 37, 345–359. https://doi.org/10.1007/s00367-017-0499-1.

Alexander, C.R., Venherm, C., 2003. Modern sedimentary processes in the Santa Monica, California continental margin: sediment accumulation, mixing and budget. Mar. Environ. Res. 56, 177–204. https://doi.org/10.1016/S0141-1136(02)00330-6.

Alizad, K., Hagen, S.C., Morris, J.T., Bacopoulos, P., Bilskie, M.V., Weishampel, J.F., Medeiros, S.C., 2016. A coupled, two-dimensional hydrodynamic-marsh model with biological feedback. Ecol. Model. 327, 29–43. https://doi.org/10.1016/j.ecolmodel.2016.01.013.

Angelini, C., van Montfrans, S.G., Hensel, M.J.S., He, Q., Silliman, B.R., 2018. The importance of an underestimated grazer under climate change: how crab density, consumer competition, and physical stress affect salt marsh resilience. Oecologia 187, 205–217. https://doi.org/10.1007/s00442-018-4112-8.

Bater, C.W., Coops, N.C., 2009. Evaluating error associated with lidar-derived DEM interpolation. Comput. Geosci. 35, 289–300. https://doi.org/10.1016/j.cageo.2008.09.001.

Benner, R., Newell, S.Y., Maccubbin, A.E., Hodson, R.E., 1984. Relative contributions of bacteria and fungi to rates of degradation of lignocellulosic detritus in salt-marsh sediments. Appl. Environ. Microbiol. 48, 36–40.

Bridgham, S.D., Megonigal, J.P., Keller, J.K., Bliss, N.B., Trettin, C., 2006. The carbon balance of North American wetlands. Wetlands 26, 889–916. https://doi.org/10.1672/0277-5212(2006)26[889. TCBONA]2.0.CO;2.

Burns, C.J., Alber, M., Alexander, C.R., 2020. Historical changes in the vegetated area of salt marshes. Estuar. Coast 1–16. https://doi.org/10.1007/s12237-020-00781-6.

Cadol, D., Elmore, A.J., Guinn, S.M., Engelhardt, K.A.M., Sanders, G., 2016. Modeled tradeoffs between developed land protection and tidal habitat maintenance during rising sea levels. PloS One 11, e0164875. https://doi.org/10.1371/journal.pone.0164875.

Cadol, D., Engelhardt, K., Elmore, A., Sanders, G., 2014. Elevation-dependent surface elevation gain in a tidal freshwater marsh and implications for marsh persistence. Limnol. Oceanogr. 59, 1065–1080. https://doi.org/10.4319/lo.2014.59.3.1065.

Cahoon, D.R., Guntenspergen, G.R., 2010. Climate change, sea-level rise, and coastal wetlands. Natl. Wetl. Newsl. 32, 8–12.

Cahoon, D.R., Lynch, J.C., Roman, C.T., Schmit, J.P., Skidds, D.E., 2019. Evaluating the relationship among wetland vertical development, elevation capital, sea-level rise, and tidal marsh sustainability. Estuar. Coast 42, 1–15. https://doi.org/10.1007/s12237-018-0448-x.

Cloern, J.E., Canuel, E.A., Harris, D., 2002. Stable carbon and nitrogen isotope composition of aquatic and terrestrial plants of the San Francisco Bay estuarine system. Limnol. Oceanogr. 47, 713–729. https://doi.org/10.4319/lo.2002.47.3.0713.

Coleman, D.J., Ganju, N.K., Kirwan, M.L., 2020. Sediment delivery to a tidal marsh platform is minimized by source decoupling and flux convergence. J. Geophys. Res. Earth Surf. 125 https://doi.org/10.1029/2020JF005558.

Coleman, D.J., Kirwan, M.L., 2019. The effect of a small vegetation dieback event on salt marsh sediment transport. Earth Surf. Process. Landforms 44, 944–952. https://doi.org/10.1002/esp.4547.

Craft, C., 2007. Freshwater input structures soil properties, vertical accretion, and nutrient accumulation of Georgia and U.S tidal marshes. Limnol. Oceanogr. 52, 1220–1230. https://doi.org/10.4319/lo.2007.52.3.1220.

Crosby, S.C., Sax, D.F., Palmer, M.E., Booth, H.S., Deegan, L.A., Bertness, M.D., Leslie, H. M., 2016. Salt marsh persistence is threatened by predicted sea-level rise. Estuar. Coast Shelf Sci. 181, 93–99. https://doi.org/10.1016/J.ECSS.2016.08.018.

Crotty, S.M., Angelini, C., Bertness, M.D., 2017. Multiple stressors and the potential for synergistic loss of New England salt marshes. PloS One 12. https://doi.org/10.1371/journal.pone.0183058.

Crotty, S.M., Ortals, C., Pettengill, T.M., Shi, L., Olabarrieta, M., Joyce, M.A., Altieri, A. H., Morrison, E., Bianchi, T.S., Craft, C., Bertness, M.D., Angelini, C., 2020. Sea-level rise and the emergence of a keystone grazer alter the geomorphic evolution and ecology of southeast US salt marshes. Proc. Natl. Acad. Sci. U.S.A. 117, 17891–17902. https://doi.org/10.1073/pnas.1917869117.

Currin, C., Newell, S., Paerl, H., 1995. The role of standing dead *Spartina alterniflora* and benthic microalgae in salt marsh food webs: considerations based on multiple stable isotope analysis. Mar. Ecol. Prog. Ser. 121, 99–116. https://doi.org/10.3354/meps121099.

D'Alpaos, A., Lanzoni, S., Marani, M., Rinaldo, A., 2007. Landscape evolution in tidal embayments: modeling the interplay of erosion, sedimentation, and vegetation dynamics. J. Geophys. Res. 112, F01008. https://doi.org/10.1029/2006JF000537.

Dame, R., Alber, M., Allen, D., Mallin, M., Montague, C., Lewitus, A., Chalmers, A., Gardner, R., Gilman, C., Kjerfve, B., Pinckney, J., Smith, N., 2000. Estuaries of the South Atlantic coast of North America: their geographical signatures. Estuaries 23, 793–819. https://doi.org/10.2307/1352999.

Day, J.W., Kemp, G.P., Reed, D.J., Cahoon, D.R., Boumans, R.M., Suhayda, J.M., Gambrell, R., 2011. Vegetation death and rapid loss of surface elevation in two contrasting Mississippi delta salt marshes: the role of sedimentation, autocompaction and sea-level rise. Ecol. Eng. 37, 229–240. https://doi.org/10.1016/j.ecoleng.2010.11.021.

Deegan, L., Garritt, R., 1997. Evidence for spatial variability in estuarine food webs. Mar. Ecol. Prog. Ser. 147, 31–47. https://doi.org/10.3354/meps147031.

Deegan, L.A., Johnson, D.S., Warren, R.S., Peterson, B.J., Fleeger, J.W., Fagherazzi, S., Wollheim, W.M., 2012. Coastal eutrophication as a driver of salt marsh loss. Nature 490, 388–392. https://doi.org/10.1038/nature11533.

DeMaster, D.J., McKee, B.A., Nittrouer, C.A., Jiangchu, Q., Guodong, C., 1985. Rates of sediment accumulation and particle reworking based on radiochemical measurements from continental shelf deposits in the East China Sea. Continent. Shelf Res. 4, 143–158. https://doi.org/10.1016/0278-4343(85)90026-3.

Donnelly, J.P., Bertness, M.D., 2001. Rapid shoreward encroachment of salt marsh cordgrass in response to accelerated sea-level rise. Proc. Natl. Acad. Sci. U.S.A. 98, 14218–14223. https://doi.org/10.1073/pnas.251209298.

Dugan, J.E., Emery, K.A., Alber, M., Alexander, C.R., Byers, J.E., Gehman, A.M., McLenaghan, N., Sojka, S.E., 2018. Generalizing ecological effects of shoreline armoring across soft sediment environments. Estuar. Coast 41, 180–196. https://doi.org/10.1007/s12237-017-0254-x.

Duran Vinent, O., Herbert, E.R., Kirwan, M.L., 2019. Lower threshold for marsh drowning suggests loss of microtidal marshes regardless of sediment supply. EarthArXiv. https://doi.org/10.31223/OSF.IO/CXVQ6.

Duvall, M.S., Wiberg, P.L., Kirwan, M.L., 2019. Controls on sediment suspension, flux, and marsh deposition near a bay-marsh boundary. Estuar. Coast 42, 403–424. https://doi.org/10.1007/s12237-018-0478-4.

Enwright, N.M., Griffith, K.T., Osland, M.J., 2016. Barriers to and opportunities for landward migration of coastal wetlands with sea-level rise. Front. Ecol. Environ. 14, 307–316. https://doi.org/10.1002/fee.1282.

Fagherazzi, S., Kirwan, M.L., Mudd, S.M., Guntenspergen, G.R., Temmerman, S., D'Alpaos, A., van de Koppel, J., Rybczyk, J.M., Reyes, E., Craft, C., Clough, J., 2012. Numerical models of salt marsh evolution: ecological, geomorphic, and climatic factors. Rev. Geophys. 50, RG1002. https://doi.org/10.1029/2011RG000359.

FitzGerald, D.M., Fenster, M.S., Argow, B.A., Buynevich, I.V., 2008. Coastal impacts due to sea-level rise. Annu. Rev. Earth Planet Sci. 36, 601–647. https://doi.org/10.1146/annurev.earth.35.031306.140139.

FitzGerald, D.M., Hughes, Z., 2019. Marsh processes and their response to climate change and sea-level rise. Annu. Rev. Earth Planet Sci. 47, 481–517. https://doi.org/10.1146/annurev-earth-082517-010255.

Friedrichs, C.T., Perry, J.E., 2001. Tidal salt marsh morphodynamics: a synthesis. J. Coast Res. 27, 7–37.

Ganju, N.K., Defne, Z., Kirwan, M.L., Fagherazzi, S., D'Alpaos, A., Carniello, L., 2017. Spatially integrative metrics reveal hidden vulnerability of microtidal salt marshes. Nat. Commun. 8, 1–7. https://doi.org/10.1038/ncomms14156.

Gedan, K.B., Kirwan, M.L., Wolanski, E., Barbier, E.B., Silliman, B.R., 2011. The present and future role of coastal wetland vegetation in protecting shorelines: answering recent challenges to the paradigm. Climatic Change 106, 7–29. https://doi.org/10.1007/s10584-010-0003-7.

Gehman, A.L.M., McLenaghan, N.A., Byers, J.E., Alexander, C.R., Pennings, S.C., Alber, M., 2018. Effects of small-scale armoring and residential development on the salt marsh-upland ecotone. Estuar. Coast 41, 54–67. https://doi.org/10.1007/s12237-017-0300-8.

Greenberg, R., Maldonado, J.E., Droege, S., McDonald, M.V., 2006. Tidal marshes: a global perspective on the evolution and conservation of their terrestrial vertebrates. Bioscience 56, 675. https://doi.org/10.1641/0006-3568(2006)56[675:tmagpo]2.0.co;2.

Hladik, C., Alber, M., 2012. Accuracy assessment and correction of a LIDAR-derived salt marsh digital elevation model. Remote Sens. Environ. 121, 224–235. https://doi.org/10.1016/j.rse.2012.01.018.

IPCC, 2013. Climate change 2013: the physical science basis. Contribution of working group I to the fifth assessment report of the intergovernmental panel on climate change. https://doi.org/10.1017/CBO9781107415324.

Kearney, M.S., Turner, R.E., 2015. Microtidal marshes: can these widespread and fragile marshes survive increasing climate–sea level variability and human action? J. Coast Res. 32, 686–699. https://doi.org/10.2112/jcoastres-d-15-00069.1.

Kirwan, M.L., Gedan, K.B., 2019. Sea-level driven land conversion and the formation of ghost forests. Nat. Clim. Change 9, 450–457. https://doi.org/10.1038/s41558-019-0488-7.

Kirwan, M.L., Guntenspergen, G.R., 2012. Feedbacks between inundation, root production, and shoot growth in a rapidly submerging brackish marsh. J. Ecol. 100, 764–770. https://doi.org/10.1111/j.1365-2745.2012.01957.x.

Kirwan, M.L., Guntenspergen, G.R., D'Alpaos, A., Morris, J.T., Mudd, S.M., Temmerman, S., 2010. Limits on the adaptability of coastal marshes to rising sea level. Geophys. Res. Lett. 37, L23401. https://doi.org/10.1029/2010GL045489.

Kirwan, M.L., Megonigal, J.P., 2013. Tidal wetland stability in the face of human impacts and sea-level rise. Nature 504, 53–60.

Kirwan, M.L., Mudd, S.M., 2012. Response of salt-marsh carbon accumulation to climate change. Nature 489, 550–553. https://doi.org/10.1038/nature11440.

Kirwan, M.L., Temmerman, S., Skeehan, E.E., Guntenspergen, G.R., Fagherazzi, S., 2016a. Overestimation of marsh vulnerability to sea level rise. Nat. Clim. Change 6, 253–260. https://doi.org/10.1038/nclimate2909.

Kirwan, M.L., Walters, D.C., Reay, W.G., Carr, J.A., 2016b. Sea level driven marsh expansion in a coupled model of marsh erosion and migration. Geophys. Res. Lett. 43, 4366–4373. https://doi.org/10.1002/2016GL068507.

Langston, A.K., Kaplan, D.A., Putz, F.E., 2017. A casualty of climate change? Loss of freshwater forest islands on Florida's Gulf Coast. Global Change Biol. 23, 5383–5397. https://doi.org/10.1111/gcb.13805.

Langston, A.K., Vinent, O.D., Herbert, E.R., Kirwan, M.L., 2020. Modeling Long-Term Salt Marsh Response to Sea Level Rise in the Sediment-Deficient Plum Island Estuary. Limnol. Oceanogr, MA. https://doi.org/10.1002/lno.11444.

Leonardi, N., Carnacina, I., Donatelli, C., Ganju, N.K., Plater, A.J., Schuerch, M., Temmerman, S., 2018. Dynamic interactions between coastal storms and salt marshes: a review. Geomorphology 301, 92–107. https://doi.org/10.1016/j.geomorph.2017.11.001.

Li, H., Yang, S.L., 2009. Trapping effect of tidal marsh vegetation on suspended sediment, Yangtze Delta. J. Coast Res. 254, 915–924. https://doi.org/10.2112/08-1010.1.

Mariotti, G., 2020. Beyond marsh drowning: the many faces of marsh loss (and gain). Adv. Water Resour. 144, 103710. https://doi.org/10.1016/j.advwatres.2020.103710.

Meade, R.H., 1982. Sources, sinks and storage of river sediments in the Atlantic drainage of the United States. J. Geol. 90, 235–252. https://doi.org/10.1086/628677.

Morris, J.T., Barber, D.C., Callaway, J.C., Chambers, R., Hagen, S.C., Hopkinson, C.S., Johnson, B.J., Megonigal, P., Neubauer, S.C., Troxler, T., Wigand, C., 2016. Contributions of organic and inorganic matter to sediment volume and accretion in tidal wetlands at steady state. Earth's Futur 4, 110–121. https://doi.org/10.1002/2015EF000334.

Morris, J.T., Sundareshwar, P.V., Nietch, C.T., Kjerfve, B., Cahoon, D.R., 2002. Responses of coastal wetlands to rising sea level. Ecology 83, 2869–2877. https://doi.org/10.1890/0012-9658(2002)083[2869:ROCWTR]2.0.CO;2.

Mudd, S.M., Howell, S.M., Morris, J.T., 2009. Impact of dynamic feedbacks between sedimentation, sea-level rise, and biomass production on near-surface marsh stratigraphy and carbon accumulation. Estuar. Coast Shelf Sci. 82, 377–389. https://doi.org/10.1016/j.ecss.2009.01.028.

Nyman, J.A., Walters, R.J., Delaune, R.D., Patrick, W.H., 2006. Marsh vertical accretion via vegetative growth. Estuar. Coast Shelf Sci. 69, 370–380. https://doi.org/10.1016/j.ecss.2006.05.041.

O'Donnell, J., Schalles, J., 2016. Examination of abiotic drivers and their influence on *Spartina alterniflora* biomass over a twenty-eight year period using Landsat 5 TM satellite imagery of the central Georgia coast. Rem. Sens. 8, 477. https://doi.org/10.3390/rs8060477.

Pennings, S., Alber, M., Alexander, C., Booth, M., Burd, A., Cai, W.-J., Craft, C., DePratter, C., Di Iorio, D., Hopkinson, C., Joye, S., Meile, C., Moore, W., Silliman, B., Thompson, V., Wares, J., 2012. South Atlantic tidal wetlands. In: Batzer, D., Baldwin, A. (Eds.), Wetland Habitats of North America: Ecology and Conservation Concerns. University of California Press, Berkeley, CA, USA, pp. 45–61.

Redfield, A.C., 1972. Development of a new England salt marsh. Ecol. Monogr. 42, 201–237. https://doi.org/10.2307/1942263.

Reed, D.J., 2002. Sea-level rise and coastal marsh sustainability: geological and ecological factors in the Mississippi delta plain. Geomorphology 48, 233–243. https://doi.org/10.1016/S0169-555X(02)00183-6.

Reed, D.J., 1995. The response of coastal marshes to sea-level rise: survival or submergence? Earth Surf. Process. Landforms 20, 39–48. https://doi.org/10.1002/esp.3290200105.

Roner, M., D'Alpaos, A., Ghinassi, M., Marani, M., Silvestri, S., Franceschinis, E., Realdon, N., 2016. Spatial variation of salt-marsh organic and inorganic deposition and organic carbon accumulation: inferences from the Venice lagoon. Italy. Adv. Water Resour. 93, 276–287. https://doi.org/10.1016/J.ADVWATRES.2015.11.011.

Schieder, N.W., Walters, D.C., Kirwan, M.L., 2018. Massive upland to wetland conversion compensated for historical marsh loss in Chesapeake Bay, USA. Estuar. Coast 41, 940–951. https://doi.org/10.1007/s12237-017-0336-9.

Schile, L.M., Callaway, J.C., Morris, J.T., Stralberg, D., Parker, V.T., Kelly, M., 2014. Modeling tidal marsh distribution with sea-level rise: evaluating the role of vegetation, sediment, and upland habitat in marsh resiliency. PloS One 9, e88760. https://doi.org/10.1371/journal.pone.0088760.

Schuerch, M., Spencer, T., Temmerman, S., Kirwan, M.L., Wolff, C., Lincke, D., McOwen, C.J., Pickering, M.D., Reef, R., Vafeidis, A.T., Hinkel, J., Nicholls, R.J., Brown, S., 2018. Future response of global coastal wetlands to sea-level rise. Nature 561, 231–234. https://doi.org/10.1038/s41586-018-0476-5.

Shepard, C.C., Crain, C.M., Beck, M.W., 2011. The protective role of coastal marshes: a systematic review and meta-analysis. PloS One 6. https://doi.org/10.1371/journal.pone.0027374.

Sousa, A.I., Lillebø, A.I., Pardal, M.A., Caçador, I., 2010. Productivity and nutrient cycling in salt marshes: contribution to ecosystem health. Estuar. Coast Shelf Sci. 87, 640–646. https://doi.org/10.1016/j.ecss.2010.03.007.

Swanson, K.M., Drexler, J.Z., Schoellhamer, D.H., Thorne, K.M., Casazza, M.L., Overton, C.T., Callaway, J.C., Takekawa, J.Y., 2014. Wetland accretion rate model of ecosystem resilience (WARMER) and its application to habitat sustainability for endangered species in the San Francisco Estuary. Estuar. Coast 37, 476–492. https://doi.org/10.1007/s12237-013-9694-0.

Syvitski, J.P.M., Vörösmarty, C.J., Kettner, A.J., Green, P., 2005. Impact of humans on the flux of terrestrial sediment to the global coastal ocean. Science 308, 376–380. https://doi.org/10.1126/science.1109454.

Temmerman, S., Govers, G., Meire, P., Wartel, S., 2003. Modelling long-term tidal marsh growth under changing tidal conditions and suspended sediment concentrations, Scheldt estuary, Belgium. Mar. Geol. 193, 151–169. https://doi.org/10.1016/S0025-3227(02)00642-4.

Thorne, K., MacDonald, G., Guntenspergen, G., Ambrose, R., Buffington, K., Dugger, B., Freeman, C., Janousek, C., Brown, L., Rosencranz, J., Holmquist, J., Smol, J., Hargan, K., Takekawa, J., 2018. U.S. Pacific coastal wetland resilience and

vulnerability to sea-level rise. Sci. Adv. 4, eaao3270 https://doi.org/10.1126/sciadv.aao3270.

Trimble, S.W., 2008. The use of historical data and artifacts in geomorphology. Prog. Phys. Geogr. Earth Environ. 32, 3–29. https://doi.org/10.1177/0309133308089495.

Trimble, S.W., 1974. Man-induced Soil Erosion on the Southern Piedmont 1700-1970. Soil Conservation Society of America, Akeny, IA, USA.

Van der Wegen, M., Roelvink, J.A., Jaffe, B.E., 2019. Morphodynamic resilience of intertidal mudflats on a seasonal time scale. J. Geophys. Res. Ocean. 124, 8290–8308. https://doi.org/10.1029/2019JC015492.

Warren, R.S., Niering, W.A., 1993. Vegetation change on a Northeast tidal marsh: interaction of sea-level rise and marsh accretion. Ecology 74, 96–103. https://doi.org/10.2307/1939504.

Watson, E.B., Szura, K., Wigand, C., Raposa, K.B., Blount, K., Cencer, M., 2016. Sea level rise, drought and the decline of *Spartina patens* in New England marshes. Biol. Conserv. 196, 173–181. https://doi.org/10.1016/J.BIOCON.2016.02.011.

Watson, E.B., Wigand, C., Davey, E.W., Andrews, H.M., Bishop, J., Raposa, K.B., 2017. Wetland loss patterns and inundation-productivity relationships prognosticate widespread salt marsh loss for southern New England. Estuar. Coast 40, 662–681. https://doi.org/10.1007/s12237-016-0069-1.

Weston, N.B., 2014. Declining sediments and rising seas: an unfortunate convergence for tidal wetlands. Estuar. Coast 37, 1–23. https://doi.org/10.1007/s12237-013-9654-8.

Wiberg, P., Zhu, Q., Coleman, D.J., Kirwan, M.L., Alexander, C.R., Alber, M., Giblin, A.E., McGlathery, K., 2018. The role of wind in controlling sediment delivery to intertidal salt marshes (poster). Ocean Sciences Meeting. The Oceanography Society, Portland, OR.

Wieski, K., Pennings, S.C., 2014. Climate drivers of *Spartina alterniflora* saltmarsh production in Georgia, USA. Ecosystems 17, 473–484. https://doi.org/10.1007/s10021-013-9732-6.

Wu, W., Biber, P., Bethel, M., 2017. Thresholds of sea-level rise rate and sea-level rise acceleration rate in a vulnerable coastal wetland. Ecol. Evol. 7, 10890–10903. https://doi.org/10.1002/ece3.3550.

Zedler, J.B., Kercher, S., 2005. Wetland resources: status, trends, ecosystem services, and restorability. Annu. Rev. Environ. Resour. 30, 39–74. https://doi.org/10.1146/annurev.energy.30.050504.144248.